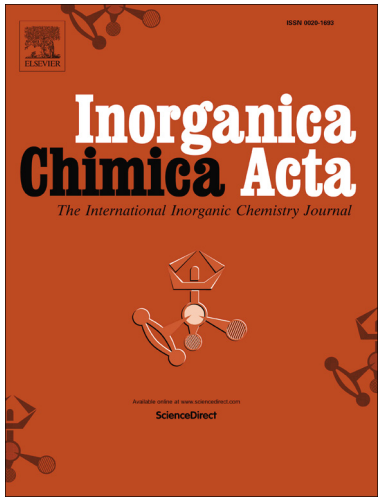

Research paper

"Novel application of simple molybdates: catalytic hydrolysis of an organophosphate neurotoxin under mild aqueous conditions"

Louis Y. Kuo, Kristina M. Dill, Yusef A. Shari'ati, Emily K. Bright, Theresa McCormick

PII: S0020-1693(17)30719-3
DOI: http://dx.doi.org/10.1016/j.ica.2017.05.007
Reference: ICA 17576

To appear in: *Inorganica Chimica Acta*

Received Date: 19 July 2016
Revised Date: 11 April 2017
Accepted Date: 6 May 2017

Please cite this article as: L.Y. Kuo, K.M. Dill, Y.A. Shari'ati, E.K. Bright, T. McCormick, "Novel application of simple molybdates: catalytic hydrolysis of an organophosphate neurotoxin under mild aqueous conditions", *Inorganica Chimica Acta* (2017), doi: http://dx.doi.org/10.1016/j.ica.2017.05.007

"Novel application of simple molybdates: catalytic hydrolysis of an organophosphate neurotoxin under mild aqueous conditions"

Louis Y. Kuo,*[a] Kristina M. Dill,[a] Yusef A. Shari'ati,[a] Emily K. Bright[a] and Theresa McCormick[b]

[a]Department of Chemistry

Lewis & Clark College

Portland, OR 97219

[b]Department of Chemistry

Portland State University

Portland, OR 97207

Abstract

A novel protocol for hydrolyzing phosphonothioate neurotoxins has been developed that uses a readily available, inexpensive and non-toxic molybdate (MoO_4^{2-}). The target organophosphate is *O,S*-diethylphenyl phosphonothioate (**1**), a model compound that has served as an analog of the chemical warfare agent VX. Molybdate-mediated hydrolysis of **1** proceeds at room temperature (pH ~7.5) and yields a relatively safe phosphonate product through P-S specific scission. This is the first report of utilizing the molybdate, MoO_4^{2-}, to degrade an organophosphate neurotoxin with turnover. A $\Delta S^{\ddagger}$ of -81.5 J/ mol·K (-19.5 cal/mol·K) indicates a bimolecular process, and ^{18}O-labelling studies show no oxygen exchange of **1** throughout the hydrolysis by $MoO_4^{2-}(aq)$. We hypothesize primarily the monomeric molybdate is the active species at pH 7.5 where a $S_N2(P)$ mechanism takes place. Density functional theory methods suggest the molybdate oxoanion serves as the nucleophile to attack phosphonothioate **1** to form a molybdate-phosphonate anhydride that subsequently hydrolyzes to the starting molybdate and phenylethyl phosphonate.

Introduction

We report the first application of the molybdate dianion (MoO_4^{2-}) [1] for hydrolyzing an organophosphate neurotoxin. Phosphonothioates (Figure 1) of the form $R^1P(O)(SR^2)(OR^3)$ are acetylcholine esterase inhibitors [2] that have applications as pesticides [3,4,5], and most notoriously as chemical warfare agents [6,7]. These compounds are extremely dangerous to human health. For example, the nerve agent VX (R^1=CH_3, R^2 = $CH_2CH_2N(iPr)_2$, R^3 = Et) has an LD_{50} = 0.015 mg/kg [8], which means that just two drops would kill an average adult.

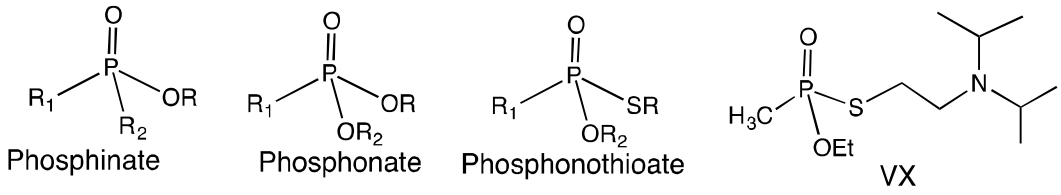

Figure 1. Structures of various organophosphorus compounds.

Organophosphate pesticide exposure has attracted increasing apprehension as a public health concern.[6] Structurally similar to related chemical warfare agents, these pesticides contain analogous P-O and P-S ligations.[6] For example, the phosphorothioate pesticide parathion [9] ($ArOP(S)(OEt)_2$) undergoes tautomerization (Scheme 1)[10] to form a product with the same P-S and P-O ligation as VX [11, 12].

Scheme 1. Tautomerization of parathion

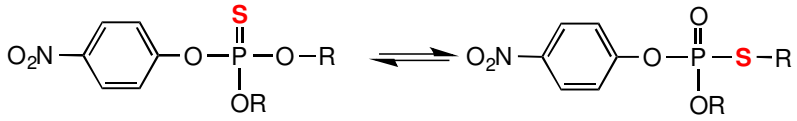

Therefore, effective protocols for breaking down phosphonothioates such as VX and common pesticides have major environmental and societal benefits.

Several efforts towards degrading phosphonothioates with discrete inorganic complexes have been reported. Lanthanide(III) – catalyzed methanolysis is an effective tool for degrading phosphonothioates, [13,14,15] and the rapid nature of this protocol has been capitalized on live nerve agent (i.e. VX) destruction [16]. The fluoride anion also hydrolyzes VX, forming an intermediate phosphonofluoridate that subsequently undergoes hydrolysis to yield a phosphonate [17].

The compound *O,S*-diethyl phenyl phosphonothioate (**1**) [18] is an analog of the chemical warfare agent VX; both 1 and VX have P-O and P-S linkages with similar hydrolytic labilities [19]. In the hydrolytic degradation of phosphonothioates, P-S scission is the preferred avenue as it yields a less toxic phosphonate. Specifically, alkaline hydrolysis of VX (and **1**) in 0.10 M NaOH proceeds 15-18% of the time through P-O scission to yield another phosphonothioate (EA 2192) that is as toxic as the starting VX (Scheme 2) [20].

Scheme 2. Alkaline hydrolysis of VX in 0.10 M NaOH yields both phosphonate (EMPA) and toxic phosphonothioate (EA 2192).

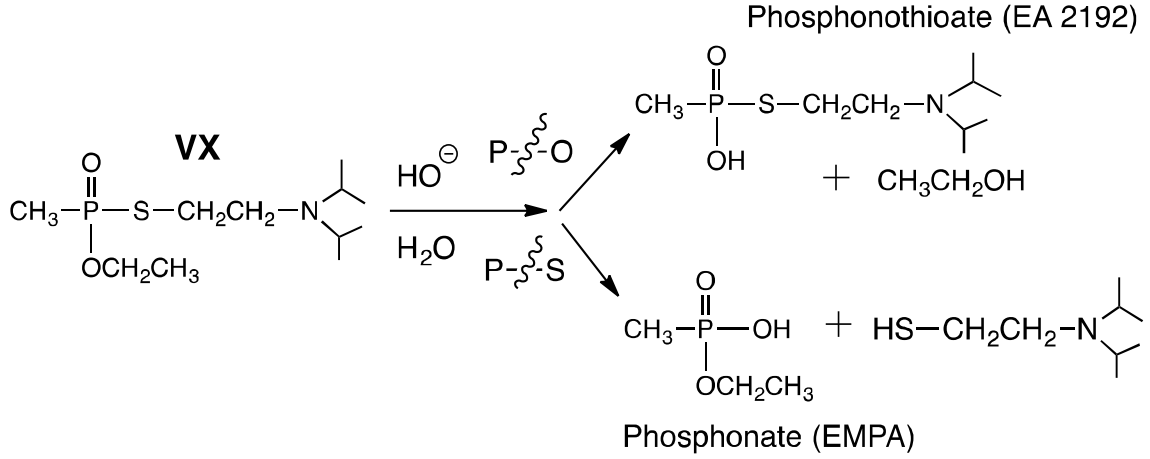

Moreover, in alkaline solution the toxic EA 2192 product is an anion that is further resistant to hydrolysis by the hydroxide nucleophile. Thus, reagents such as iodosobenzoate (IBA) [21,22] that promote P-S scission of phosphonothioates are desirable complexes for degrading organophosphate neurotoxins.

The only molybdenum complexes that hydrolyze phosphonothioates are the metallocenes of the form Cp_2MoCl_2 (Cp = η^5-C_5H_5) [23]. Their hydrolytic activity is characterized by P-S specific scission of phosphonothioate **1** under mild conditions (pH 7, 30 °C) [24]. However, the thiophilic Mo(IV) results in strong Cp_2Mo^{IV}-SEt ligation [25,26,27] with the alkylthiolate leaving group of **1** [24]. The subsequent $Cp_2Mo(SEt)_2$ adduct (Scheme 3) is inert and prevents additional hydrolysis of **1** by Cp_2MoCl_2(*aq*); the metallocene *functions not as a catalyst but merely as a reactant*.[28].

Scheme 3. Hydrolysis of **1** by Cp_2MoCl_2(*aq*).

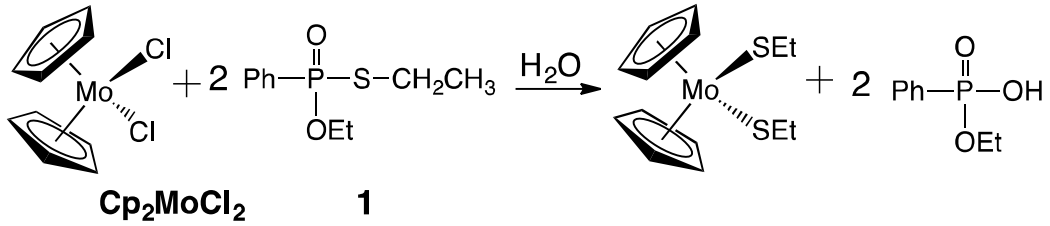

Cp_2MoCl_2 **1**

Therefore, to improve phosphonothioate hydrolysis by molybdenum complexes, we require an inexpensive and air-stable system that does not have a soft thiophilic center [29]. To that end, we report the activity of the molybdate dianion, MoO_4^{2-}, towards **1** hydrolysis with the desired P-S specific bond scission [30]. This report delineates the chemistry of phosphonothioate hydrolysis by the simple molybdate dianion. This work was prompted by prior results that showed polyoxomolybdates and MoO_4^{2-} hydrolyze organophosphates [31,32,33] and simple peptides [34]. Early molybdate-promoted hydrolysis of organic phosphate bonds (i.e. ATP, creatine phosphate, fructuose-6-

phosphate, and acetyl phosphate) were done under acidic conditions [35,36,37]. In that connection, molybdates were also shown to affect several acid phosphatases (i.e. yeast and tomato) [37,38], and this was even implicated as a possible metabolic role for molybdenum [39,40,41,42].

Results and Discussion

Our studies of the molybdate-mediated hydrolysis of **1** begin by showing that MoO_4^{2-} hydrolyzes **1** with the desired P – S bond scission, followed by results showing (1) the absence of leaving group coordination to the molybdate dianion (i.e. $MoO_4^{2-}(aq)$ functions as a catalyst), (2) structure-activity relationship studies with modified phosphonothioates, (3) the outcome of tracking studies with ^{18}O-labeled **1**, and (4) computational results that suggest a $S_N2(P)$ pathway. ^{31}P NMR spectroscopy (Figure 2) shows formation of only one product with a singlet at 15 ppm consistent with phosphonate formation. The absence of a phosphonothioate signal (~33 ppm) [18] clearly shows only P – S scission, and this ^{31}P NMR profile is the main spectral feature throughout this report.

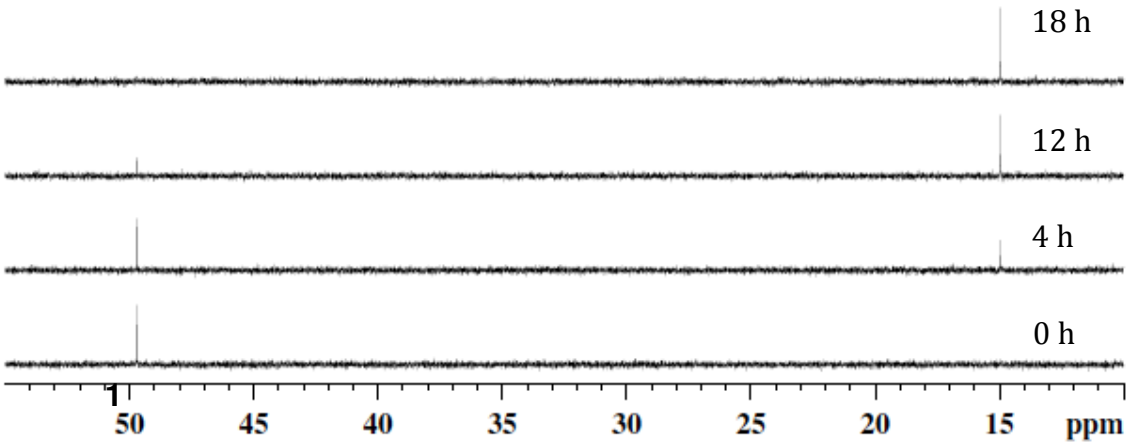

Figure 2: ^{31}P NMR spectrum of the hydrolysis of **1** (16 mM) by excess MoO_4^{2-} (1.0 M) in MOPS (1.0 M, pH 7.5 (20% D_2O), 30 ^oC) that shows only one phosphonate product (15 ppm), resulting from selective P-S scission. A wider spectral expansion from -20 to 120 ppm shows no additional ^{31}P NMR signals.

In addition, 2.0 M NaCl accomplishes no hydrolysis of **1**, and $LiClO_4$ was also inactive in degrading **1** under similar pH and temperature conditions. Finally, under these conditions (pH 7.5 MOPS buffer, 30 ^oC), **1** is stable for at least a month; this lack of background auto-hydrolysis indicates MoO_4^{2-} is responsible for promoting **1** hydrolysis.

In addition to the specific P – S scission, a proof-of-concept result shows MoO_4^{2-} can function as a catalyst for hydrolyzing **1**. Our initial question asks if the Mo(VI) center in MoO_4^{2-} would be poisoned by the ethanethiolate leaving group in **1** hydrolysis. Accordingly, the ^{13}C NMR signal of sodium ethanethiolate upon addition of Na_2MoO_4 in H_2O (pH 7.5 MOPS buffer with 20% D_2O) remained unchanged, thus indicating no interaction between the ethanethiol and MoO_4^{2-}. In this connection, *we found **1** is hydrolyzed by Na_2MoO_4 in H_2O even when excess phosphonothioate was used. Specifically, 1 mM of Na_2MoO_4 successfully hydrolyzes 15 mM of **1** in pH 7.5 at 30^oC with only P-S scission with the same ^{31}P NMR as Figure 2.* Prior results with the organometallic molybdenum(IV) metallocene showed no such turnover [24,28]. This is the first evidence of a molybdenum complex (of any oxidation state) that exhibits catalytic hydrolysis of a phosphonothioate neurotoxin under mild aqueous conditions. While the hydrolysis is impractically slow at 30 ^oC (6 days for just 15 equivalents of **1** – turnover frequency of 2/day), the ^{31}P NMR indicates the desired P-S scission. This is evident from the presence of just one product signal (15 ppm), which is consistent with

phosphonate production; no evidence of the toxic phosphonothioate product (33 ppm) [18] is observed.

When the ^{13}C – enriched phosphonothioate *O*-ethyl *S*-^{13}methyl phenyl phosphonothioate (16 mM) was hydrolyzed by excess MoO_4^{2-} (1.0 M), only free methanethiol (confirmed through authentic addition) was formed, as shown with ^{13}C NMR (Figure 3). There is no indication of metal coordination, nor methylsulfate formation (i.e. no signal at 38 ppm for $CH_3SO_3^-$). Only the presence of methyl disulfide at 21.3 ppm is evident, which comes about from the air oxidation of the released methanethiol. The evidence taken together, which includes the stoichiometry (1eq MoO_4^{2-}:15 eq **1**) and the aformentioned ^{13}C and ^{31}P NMR results suggest the molybdate does not coordinate to any of the hydrolytic products and therefore remains as MoO_4^{2-} (*aq*) throughout the reaction. This allows it to hydrolyze **1** multiple times albeit slowly.

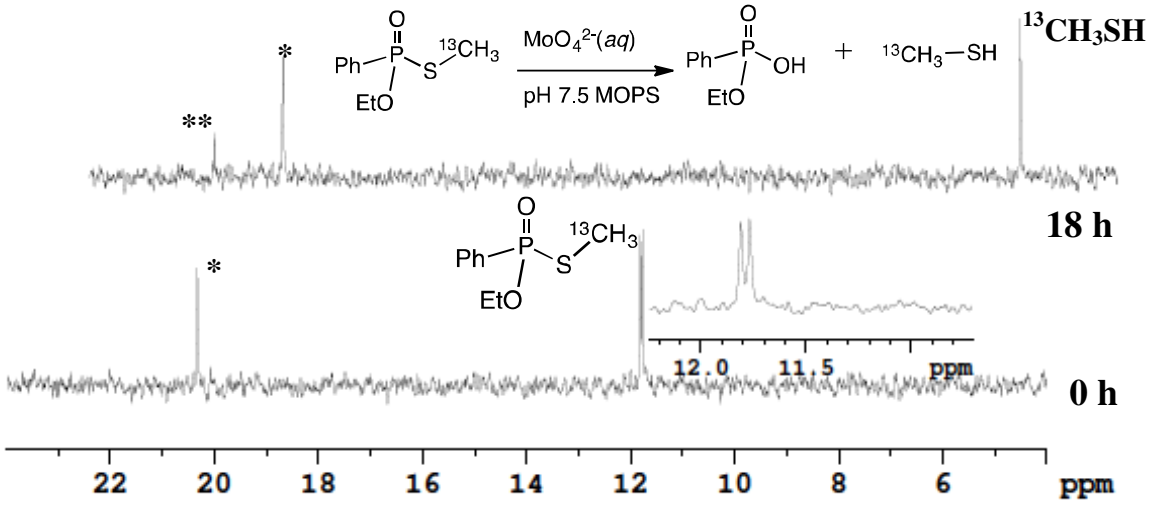

Figure 3: ^{13}C NMR spectrum of the hydrolysis of *O*-ethyl *S*-^{13}methyl phenyl phosphonothioate (^{13}C-enriched on the methyl carbon at 11.8 ppm; $^2J_{PC}$ = 6.5 Hz) with MoO_4^{2-} that shows production of only free methanethiol (5.7 ppm). Hydrolysis (30 ^oC) was done on 16 mM of the ^{13}C-enriched phosphonothioate (2 µL) in 1 mL MOPS* buffer (pH 7.5) and 1.0 M MoO_4^{2-}. The presence of only methanethiol and the oxidized dimethyl sulfide (**) indicates no molybdenum coordination to the leaving group.

Initial results of **1** hydrolysis by MoO_4^{2-} indicate that the reaction is first order in MoO_4^{2-} (Supporting Information S1). There was no concentration dependency in [**1**] when [MoO_4^{2-}] is fixed, but we suspect this may be due to the limited water solubility of the phosphonothioate, because when [**1**] > 20 mM the solution was cloudy from droplets of **1**. Therefore, saturation kinetics with varying phosphonothioate concentration is problematic for attaining any Michaelis-Menten values. Addition of alcohols or THF to increase **1** solubility is also poses data interpretation issues, as these additives may affect the speciation and solubility of the molybdates.

Operationally, the optimum pH (6.9 to 7.5) for these experimental conditions favors the formation of the monomeric molybdate in terms of the quickest kinetics runs. The speciation of polyoxomolybdates is known to be pH sensitive [44, 45] wherein the heptamer $Mo_7O_{24}^{6-}$ and octamer $Mo_8O_{26}^{4-}$ exist primarily in the pH range of 5.5 – 6.5 and <4.0, respectively. Indeed, acidification of MoO_4^{2-} results in formation of the heptamer and octamer polyoxomolybdates, in which the speciation was previously modeled (Supporting information S2) [32]. Specifically, equilibrium calculations show that the monomeric MoO_4^{2-} (400 mM) is the main species at pH > 7.5. In this connection, we found that the maximal rate of **1** hydrolysis by 400 mM MoO_4^{2-} occurred at pH 6.9. Interestingly, Parac-Vogt and coworkers also found that the hydrolysis of dipeptides by MoO_4^{2-} reached its maximal rate at pH 6.9 [31], which implicated the active species as the monomeric molybdate. To that end, the pH value of 7.5 was chosen in our studies to ensure that monomeric MoO_4^{2-} was the key species for hydrolyzing **1**. Any work above pH 8.5 would be problematic as the phosphonothioate undergoes spontaneous alkaline hydrolysis. We do not discount the possibility that at this pH an equilibrium exists

between the major monomeric (MoO_4^{2-}) species and with any of the aforementioned (minor) polymeric molybdates that exist in the acidic range. It should be noted that below pH 6 the hydrolysis of **1** by $MoO_4^{2-}(aq)$ is not detectable which suggests these polymeric molybdates are poor candidates for phosphonothioate hydrolysis.

We set out to examine possible structure-activity relationships by steric parameters of the phosphonothioate substrate. A similar investigation [24] was made with the thiophilic molybdenum metallocene (Cp_2MoCl_2). In this past study several phenyl phosphonothioates were made wherein the alkylthiolate was varied. In this work [24] the hydrolysis rates of four different phenyl phosphonothioates, (PhP(O)(OEt)(SR); R = CH_3, Et, Pr and ^{i}Pr) by $Cp_2MoCl_2(aq)$ correlate well with the Taft parameter, (Es) of the alkylthiolate (SR) leaving group. The Taft parameter, a quantitative steric indicator, is derived from the hydrolysis rates of alkyl benzoates [46]. In addition, this correlation may also depend on the acidity of the alkylthiolate leaving group (i.e. pKa of RSH) [47]. We saw that both factors affect the rates of phosphonothioate hydrolysis by the thiophilic molybdenum metallocene Cp_2MoCl_2. There is a marked decrease in the rates of phosphonothioate hydrolysis as the size of the leaving group increases and as the acidity of RSH decreases.

In a similar study, we sought to determine if a similar relationship existed for the molybdate– mediated hydrolysis of these same phenyl phosphonothioates (Figure 4).

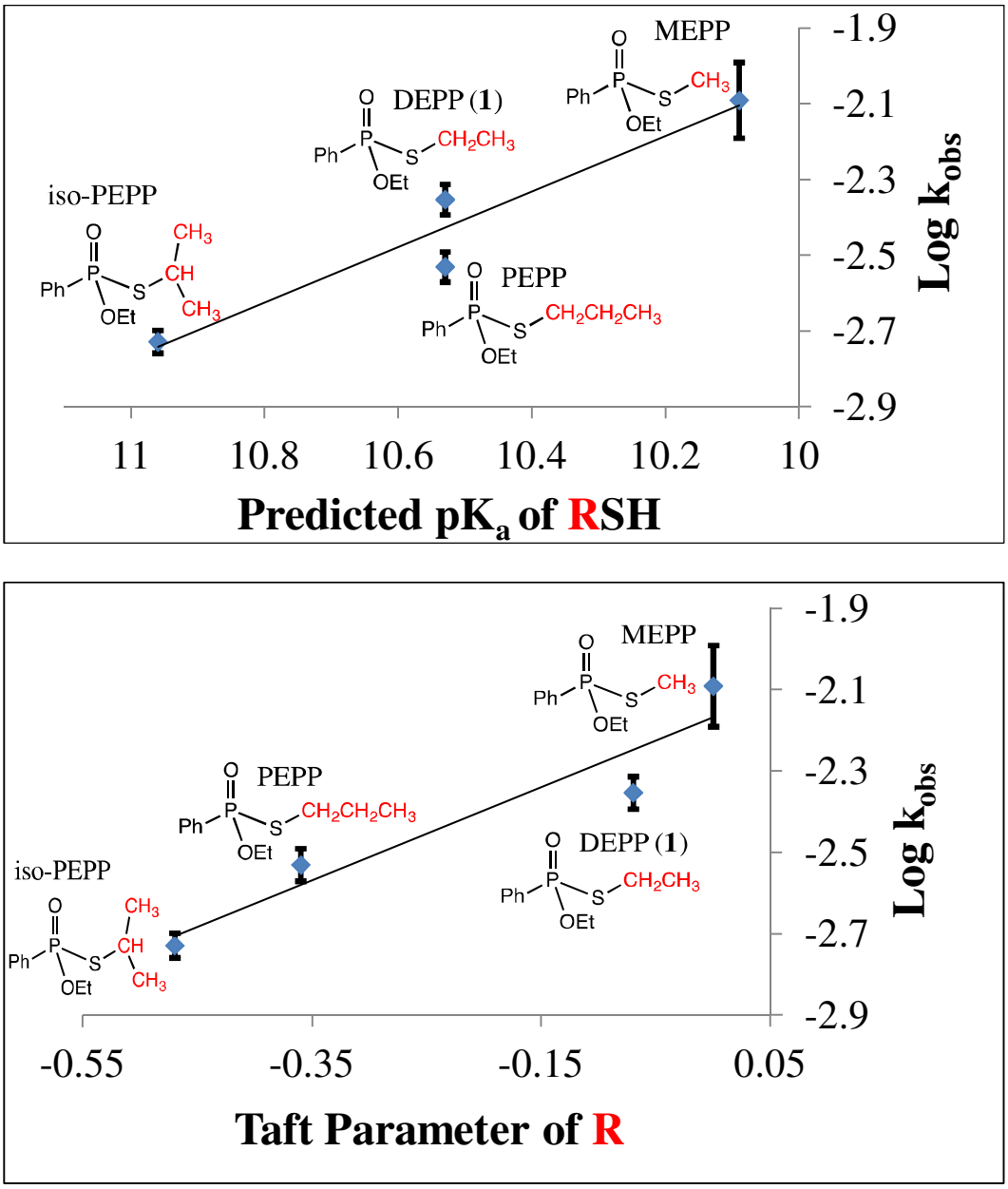

Figure 4: The hydrolysis of various *S*-alkyl *O*-ethyl phenyl phosphonothioates (16 mM) by 1.0 M MoO_4^{2-} (30°C, pH 7.5, 1.0 M MOPS) shows that there is a correlation between the size of the alkylthiolate leaving group and the rate of hydrolysis. Predicted pK_a was taken from reference [48]. MEPP, DEPP (**1**), PEPP and iso-PEPP represent methyl, ethyl, n-propyl and isopropyl thiolate groups, respectively.

Indeed, there is a strong dependence on the size and acidity of the alkylthiolate leaving group for the hydrolysis of **1** by MoO_4^{2-}(*aq*). Given the absence of any reaction between

$MoO_4^{2-}$and ethanethiol, it is unlikely that there would be an interaction between the Mo(VI) oxide and the sulfur linkage of the alkylthiolate leaving group. Therefore, the trend in Figure 4 shows that the hydrolytic reaction is sensitive to the leaving group ability (acidity) of the alkylthiolate. This is further supported with computational calculations discussed at the end of this report.

Thermodynamic measurements (Table 1) of **1** hydrolysis were undertaken to determine the molecularity of the rate determining step. The 60 degree temperature range yielded a clean Arrhenius plot (Supporting information S3) that gave a $\Delta S^{\ddagger}$ of -81.5 J/ mol·K (-19.5 ±0.3 cal/mol·K). This large negative value indicates a bimolecular rate determining step, or one that goes through an ordered transition state. A $\Delta S^{\ddagger}$ of -316 J/ mol·K (-75.4 cal/mol·K) was measured for the $Mo_7O_{24}^{6-}$ – catalyzed hydrolysis of 2-hydroxypropyl-4-nitrophenyl phosphate [32], a model for RNA. The more positive entropy of activation in our study is consistent with a smaller molybdenum catalyst and with an organophosphate substrate with fewer degrees of rotation; the path to the transition state requires less entropy change. Interestingly, our $\Delta S^{\ddagger}$ and $\Delta H^{\ddagger}$ values are not dramatically different from the molybdate-promoted hydrolysis of *p*-nitrophenyl acetate [49], even though that latter reaction ($\Delta H^{\ddagger}$ = 15.8 ±0.1 cal/mol, $\Delta S^{\ddagger}$ = -17.4 ±0.4 cal/mol·K) was (1) done under different conditions, (2) with a different leaving group, and (3) on a carboxylic acid ester substrate. We wanted to track the fate of the terminal P=O oxygen to see if it is lost in the hydrolysis of **1** by MoO_4^{2-}(*aq*); this would help support a mechanistic hypothesis. As such, diethyl phenyl phosphonite was hydrolyzed with 25% enriched ^{18}O water followed by tautomerization to the *O*-ethyl phenyl *H*-phosphinate (Scheme 4 and Supporting information S4) [50]. Subsequent sulfur insertion [51] in the presence of

dicyclohexylamine yielded the ammonium salt of the *O*-ethyl phenyl phosphonothioate. Finally, nucleophilic substitution with ethyl iodide [18] resulted in the ^{18}O label on the terminal P=O bond of **1**. This was manifested in two ^{31}P signals (3:1) displaced by a 0.03 ppm isotopic shift [52, 53]. In this connection, ^{31}P NMR was used to track the fate of the ^{18}O label during the hydrolysis of **1**.

Scheme 4. Synthesis of ^{18}O-labelled phosphonothioate **1**

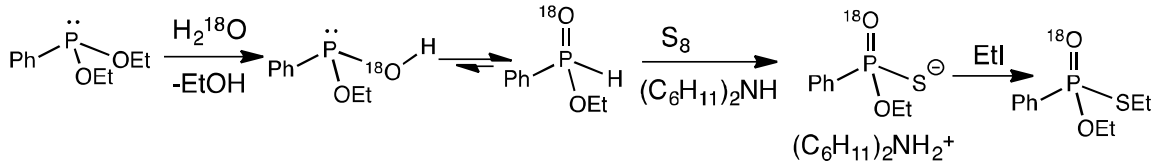

Hydrolysis of **1** in 25% ^{18}O-labelled *water* (not ^{18}O-labelled **1**) with 1.0 M MoO_4^{2-} yields the final phosphonate (14.6 ppm) with a 0.03 ppm displacement (3:1 ratio) indicative of ^{18}O incorporation into the ethyl phenyl phosphonate product (Supporting information S5). This underscores the validity of using ^{18}O-incorporation as a method to track the fate of the terminal oxygen of **1**. In this connection, ^{18}O-labelled **1** was used with MoO_4^{2-} (*aq*) and Figure 5 shows the ratio of the two ^{31}P signals of the phosphonate (15 ppm) was identical to the starting phosphonothioate at 49.7 ppm. If there is significant P-O scission of the P=^{18}O bond, then there would be a diminution in the upfield ^{31}P signal. The reverse ^{18}O – labeling where the oxygen-18 is installed on the molybdate is problematic given the rapid oxygen exchange of MoO_4^{2-} with the water solvent [54].

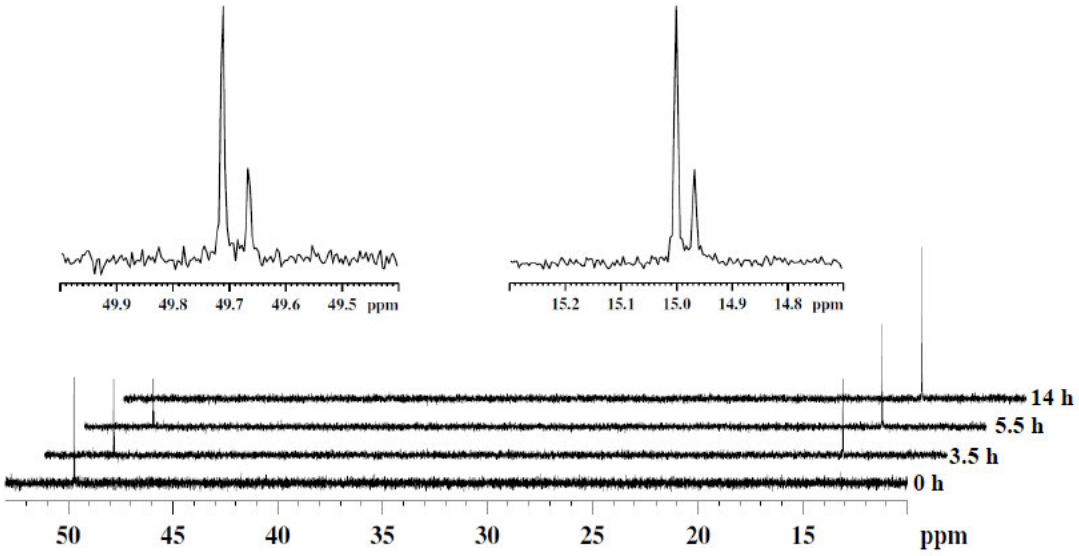

Figure 5: Hydrolysis (pH 7.5 buffer) of ^{18}O-labelled **1** (16 mM) by 1.0 M MoO_4^{2-} shows no oxygen exchange of the P=O functionality when hydrolyzed by excess molybdate. The 0.03 ppm upfield displacement results from the P=^{18}O bond, and the 3:1 ratio of integrals represent P=^{16}O to P=^{18}O, respectively. This ratio remains unchanged from the starting phosphonothioate (**1** at 49.9 ppm) to the phosphonate product (15 ppm).

This clearly indicates that no oxygen exchange took place for the P=O functionality in the presence of the MoO_4^{2-} *(aq)*.

In terms of a plausible mechanism for **1** hydrolysis by the molybdate the amphoteric character of the Mo=O bond (i.e. [Mo=O ↔ Mo^+–O^-]) may allow it to act as a nucleophile in catalyzing the hydrolysis of **1**. Indeed, DFT calculations on vanadate-catalyzed hydrolysis of peptides proposed that hydrolysis occurs via the amphoteric V=O bond [55, 56]. In this scheme the vanadate oxoanion attacks the electropositive carbon to form a tetrahedral intermediate, which is stabilized through intramolecular hydrogen bonding. Support for this model comes from prior synthetic reports that used MoO_2Cl_2 as a catalyst for nucleophilic acyl substitutions in organic solvents [57, 58]. In this work, the [Mo=O ↔ Mo^+–O^-] functionality acts as an oxoanion nucleophile that attacks the electrophilic carbon of an anhydride (Scheme 5).

Scheme 5. Mechanism for anhydride transesterification in which the [Mo=O ↔ Mo^{+}–O^{-}] functionality acts as an oxoanion nucleophile. Taken from references 57 and 58

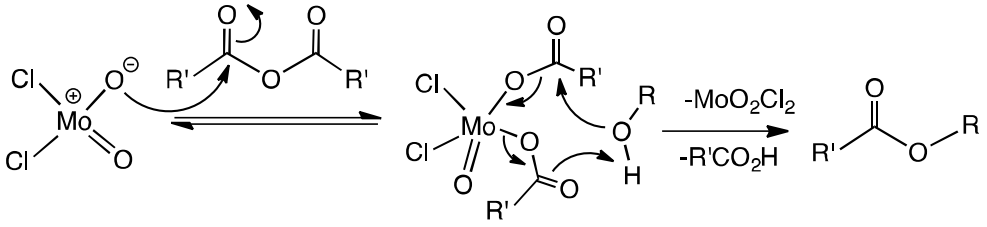

Experimental results confirmed the existence of a molybdate-carboxylate intermediate ($MoOCl_2(O_2C^tBu)_2$) resulting from the molybdenum oxoanion attacking the electrophilic carbon of pivalic anhydride. This short-lived molybdocarboxylate anhydride undergoes subsequent esterification with an alcohol. Such a route may exist for MoO_4^{2-}– catalyzed hydrolysis of **1**. In this scenario (Scheme 6), the oxoanion of the molybdate first attacks ($S_N2(P)$) the phosphonothioate to form a molybdate-phosphonate anhydride (**2**). This is followed by rapid hydrolysis to regenerate the molybdate and phosphonate product.

Scheme 6. Mechanism for phosphonothioate **1** hydrolysis in which an initial $S_N2(P)$ is followed by rapid hydrolysis of the molybdate-phosphonate anhydride.

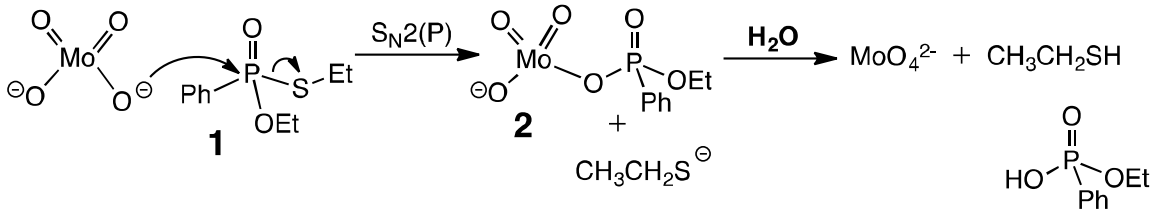

Molybdate-phosphate anhydrides yield distinctive ^{31}P NMR signals that have provided diffusion coefficients for molecular weight determinations through DOSY [32,59]. In this prior investigation by Parac-Vogt and coworkers, the heptamer $Mo_7O_{24}^{6-}$ was found to hydrolyze anionic 4-nitrophenylphosphate (NPP). This hydrolysis proceeded via $(NPP)_2Mo_5O_{21}^{4-}$ and $(NPP)_2Mo_{12}O_{36}(H_2O)^{4-}$ complexes that were seen as intermediate ^{31}P signals which were characterized through DOSY. In our studies, no

intermediate ^{31}P signal has been observed in the molybdate-mediated hydrolysis of the neutrally charged phosphonothioate. This nucleophilic molybdate mechanism (Scheme 6) cannot be ruled out, as it is possible the intermediate phosphonomolybdate (**2**) is hydrolytically unstable. Furthermore, there is a distinction between this work and the aforementioned prior study. In the prior studies the interaction was between a polyoxomolybdate and an anionically charged phosphate, but this current work is between a monomeric molybdate and a neutrally charged phosphonothioate. Indeed, Byers and coworkers [49] found that the molybdate anion is an effective nucleophile for the hydrolysis of activated carboxylic esters [49]. In addition, our $\Delta S^{\ddagger}$ is close in value to that reported by Byers for the molybdate-promoted nucleophilic attack on carboxylic esters. In summary, the $S_N2(P)$ scenario set in Schemes 6 is consistent with the reaction order, the absence of oxygen exchange on **1** and thermodynamic experimental results. The first order dependence in $[MoO_4^{2-}]$ indicates the importance of the oxoanion pathway that uses the nucleophilic Mo=O bond to attack a neutral substrate. Moreover, the large negative entropy of activation of -81.5 J/ mol·K (-19.5 cal/mol·K) is also consistent with nucleophilic (i.e. bimolecular) attack of MoO_4^{2-} on phosphonothioate **1**

The hypothesized pathway in Scheme 6 was modeled with density functional theory methods (water as the solvent) in a two-step process as shown in Figure 6. This commences with the initial $S_N2(P)$ attack by the molybdate dianion on **1** to yield the phosphonomolybdate anhydride intermediate **2**. As such, DFT calculations reveal a transition state that had a reasonable vibration (i.e. one imaginary frequency) connecting reactants MoO_4^{2-} + **1** with **2** + EtS^- (first step of Scheme 6). Subsequent hydrolysis of

anhydride intermediate **2** was best effected with hydroxide attack that yielded intermediate **3.**

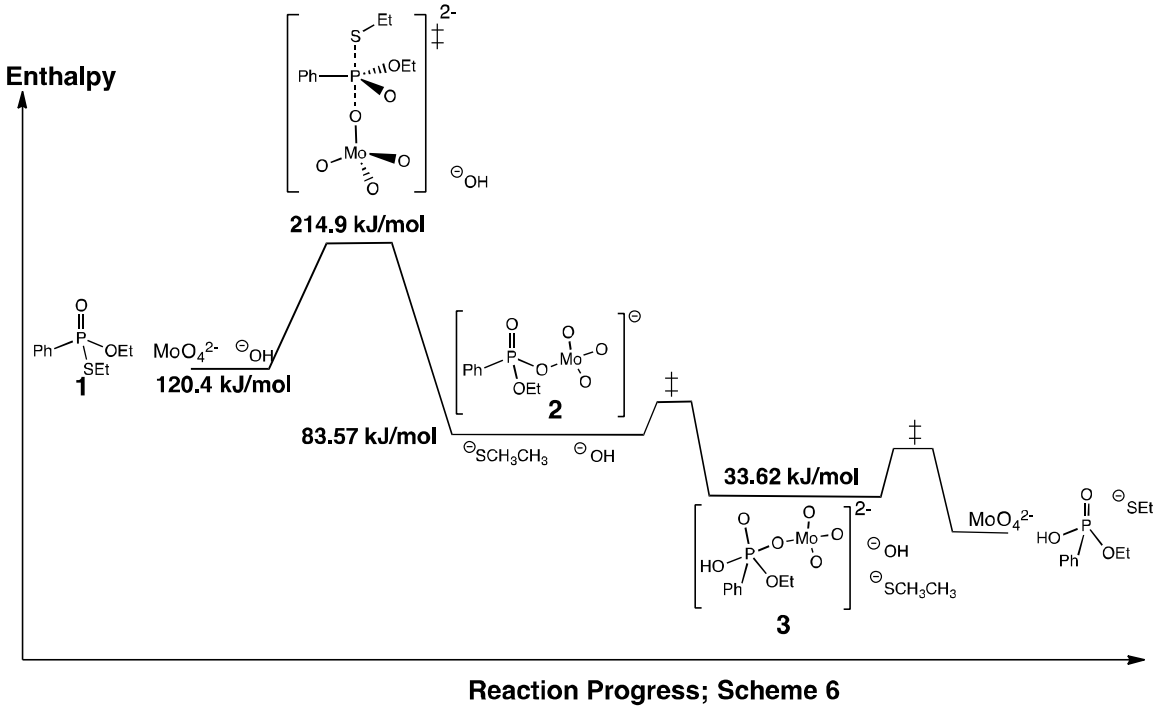

Figure 6: Reaction coordinate diagram for molybdate $S_N2(P)$ attack on **1** that delineates scheme 6 as determined through DFT calculations modeled with implicit water solvent. Energies are sum of electronic and thermal enthalpies for the compounds at each step based on an overall balanced reaction. The lowest combined energy were the final products (MoO_4^{2-}, $^-$SEt and PhP(O)(HO)(OEt) that was set to zero, all other energies are relative to this. Supporting information has full calculation results from a B3LYP optimization using a 6-31+G(d)/LanL2DZ split basis set.

Although compound **3** resembles the transition state structure of hydroxide attack, frequency calculations suggest **3** as an intermediate structure. Various attempts to model **3** as a transition state did not yield an imaginary frequency consistent with hydroxide nucleophilic attack on **2** in a $S_N2(P)$. Moreover, water attack on **2** yielded only nonsensical intermediate structures for the breakdown of **2**.

Experimentally, we see the $S_N2(P)$ yields exclusively P – S scission, and this is further supported through DFT calculations that indicate a relatively stronger P – O bond in phosphonothioate **1**. Energy calculations on **1** as a function of P – SEt and P – OEt bond lengths (Figure 7) show a deeper energy well for the P – OEt linkage. This suggests the P – O bond is stronger (by 55 kJ/mol) than the P – S bond that results in exclusive P – S scission upon hydrolysis.

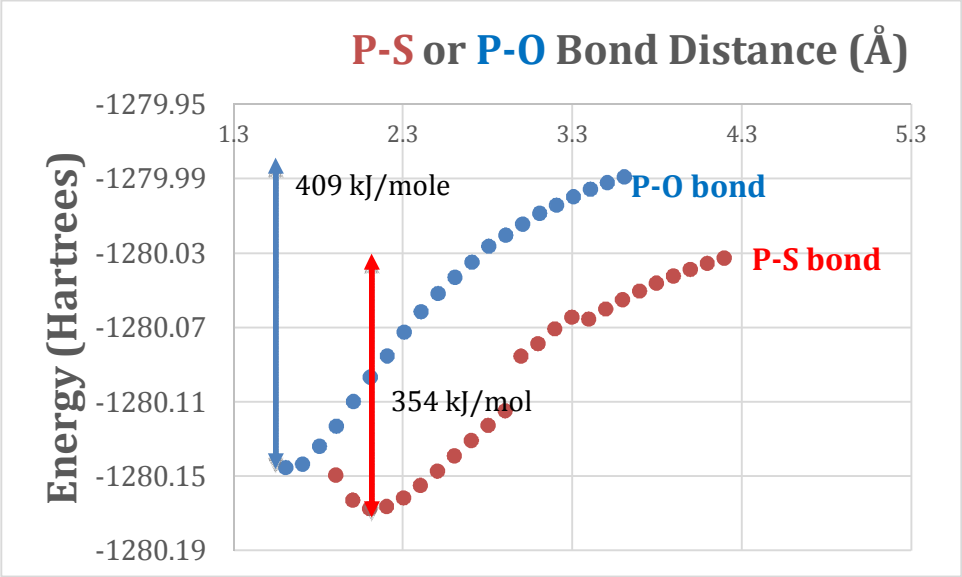

Figure 7: Molecular potential energy curve for P – SEt and P – OEt bond stretches on phosphonothioate **1** that shows the P – O bond is stronger than the P – S bond by 55.1 kJ/mol. This is consistent with experimental results that show exclusive P –S scission of **1** upon hydrolysis promoted by MoO_4^{2-}.

While the $S_N2(P)$ pathway for **1** hydrolysis appears to be the likely route for this phosphonothioate degradation by MoO_4^{2-}, other pathways cannot be completely discounted. One such route treats the Mo(VI) of MoO_4^{2-} as a Lewis acid that directly bonds to the oxygen of the P=O functionality of **1**. This alternate route is elaborated in supporting information S6, but DFT calculations were unsuccessful in optimizing any of

the proposed structures. Any minimized structure had the molybdate completely displaced (i.e. unbonded) from **1**.

Conclusion

We report the first example of catalytic phosphonothioate hydrolysis by the molybdate dianion. The title phosphonothioate (**1**) is an analog of neurotoxins such as the chemical warfare agent VX, and its hydrolysis proceeds with selective (and desired) P – S scission under mild (pH 7.5 and 30 ^{o}C) aqueous conditions with a readily available and safe metal oxide. The high oxidation Mo(VI) precludes metal coordination to the alkylthiolate leaving group, thus preserving the molybdate species and providing turnover in hydrolysis. ^{18}O labeling studies on **1** indicate no exchange with the P=O functionality on the phosphonothioate substrate. In addition, there is a strong rate dependency on the acidity of the phosphonothioate leaving group, and the activation parameters indicate a bimolecular process. A possible mechanistic route entails nucleophilic attack by MoO_4^{2-} on the phosphonothioate through a $S_N2(P)$ process; Lewis acid activation by Mo(VI) on the P=O functionality of **1** for water hydrolysis cannot be ruled out. Future studies will create other molybdenum(VI) systems that yield faster hydrolytic rates.

EXPERIMENTAL

CAUTION: The phosphonothioates are known neurotoxins and all experimental work was done with gloves in well-ventilated hoods. In addition, all glassware exposed to the phosphonothioates was bleached overnight prior to base bath cleaning to oxidize any of the phosphonothioates. It is highly recommended that

these phosphonothioates be synthesized and used on a microscale to minimize release and exposure. All phosphonothioates were stored below – 5.0 ^{o}C and allowed to warm to RT prior to kinetic runs

Equipment and supplies

All NMR spectra (^{13}C, ^{31}P, and ^{1}H) were acquired using a Bruker Advance-300 MHz NMR spectrometer at 75.468 MHz, 121.495 MHz, and 300.130 MHz respectively, and pH measurements were done with a Vernier pH probe. The pH readings in 20% D_2O were uncorrected. The dichlorophenylphosphine and precursors to the phosphonothioates were purchased from TCI America (Portland, OR), and the sodium molybdate was obtained from Mallinckrodt Chemical Works. The ^{18}O labeled H_2O and diethylphenyl phosphonate were purchased from Aldrich (Milwaukee, WI) and used as received. The MOPS (3-(N-morpholino)propanesulfonic acid) and MOPS salt were purchased from Sigma. All phosphonothioates in Figure 4 were made according to prior literature protocols [24].

Synthesis of ^{18}O-labelled phosphonothioate (**1**)

The synthesis started with the anaerobic hydrolysis of diethylphenyl phosphonite (2.0 mL, 9.8 mmole) in 1 mL of 25% ^{18}O labeled H_2O (56 mmole); the water was purged with Ar for ~3 min to minimize oxidation of the phosphonite. This hydrolysis is known to yield the *O*-ethyl phenyl phosphinate via the tautomerization shown in scheme 4 [51]. After 10 h of stirring at room temperature, the water was evaporated off under vacuum leaving behind 1.20 g (7.0 mmole, 71% yield) of an oily residue with ^{1}H and ^{31}P NMR

spectral features consistent with literature reports of *O*-ethyl phenyl phosphinate [18,43]. ^{1}H NMR ($CDCl_3$): δ 1.4 (t, 3H, O-CH_2-C**H$_3$**), 4.2 (dq, 2H, O-C**H$_2$**-CH_3), 7.52 (m, 2H, meta), 7.6(t, 1H, para), 7.75 (dd, 2H, ortho), 7.6 (s, 1H, P-**H**, $^{1}J_{PH}$ = 550 Hz). ^{31}P NMR ($CDCl_3$): δ 24.6 (Supporting information S6). Completion of the synthesis of ^{18}O – labeled **1** followed the protocol set by DeBruin [18] on a microscale [24]. This began with sulfur addition to the hydrogen phosphinate (0.80 g, 4.6 mmole) in 10 mL dicyclohexylamine. A white precipitate was isolated and dried which was then subjected to nucleophilic displacement with excess iodoethane (1.0 mL, 12.4 mmole) in 5 mL hexane (18 h). Evaporation of the hexane in vacuo left behind only 180 mg (0.78 mmole) of the ^{18}O – labeled phosphonothioate **1**: 17% overall yield. ^{1}H NMR ($CDCl_3$): δ 1.3 (t, 3H, O-CH_2-C**H$_3$**), 1.4 (t, 3H, S-CH_2-C**H$_3$**), 2.8 (q, 2H, S-C**H$_2$**-CH_3), 4.2 (q, 2H, O-C**H$_2$**-CH_3), 7.5 (m, 3H, meta and para), 7.9 (d, 2H, ortho). ^{31}P NMR ($CDCl_3$): δ 44.7.

Kinetics of **1** hydrolysis

All kinetic runs, with the exception of the pH dependency (*vide infra*), were done in a total volume of 1.0 mL of 1 M MOPS buffer (pH 7.5; 20% D_2O for deuterium lock) within an NMR tube. Sodium molybdate (0.242 g, 1.00 mmol, 1.00 M) was added and allowed time to completely dissolve wherein the pH rose to 7.5. The phosphonothioate was then added to give a molybdate to phosphonothioate ratio of 62:1 (in the case of **1** this was 2.0 μL of **1** (0.016 mmole)). *This high ratio guaranteed pseudo-first order kinetics that could be completed in less than 18 h at 30 ^{o}C.* ^{31}P spectra were taken with 32 scans and a delay of 2 seconds between each scan, at 20-minute intervals. Integration of the peaks of phosphonothioate starting materials and phosphonate products allowed for

tracking of their relative concentrations. The fraction of remaining phosphonothioate versus time was plotted and fitted to an exponential decay (first order kinetics) in Excel to 95% completion (Supporting information S7-Figure 4 and S8-Arrhenius plot). It was found that reducing the delay to 0.1 sec made no difference in the rates of hydrolysis.

Computational Details

All molecules in Figure 6 were built from GaussView [44], and full optimization on all structures were carried using the DFT model on Gaussian 09 [45] with the B3LYP functional [46, 47, 48]. The chosen basis sets were 6-31+G(d) [49, 50, 51] basis set for H, C, S, O atoms and LanL2DZ basis set [52,53] for the Mo atom. A polarizable continuum water model was used with the CPCM key word [54, 55]. All structure geometries were first optimized prior to frequency calculations to check for negative frequencies. The sum of electronic and thermal enthalpies was also taken from this (frequency) calculation for use in generating the reaction coordinate diagrams. The transition-state structure for the **1** + MoO_4^{2-} → **2** process was generated by optimizing the structure of the transition state using the Berney algorithm. The frequency calculation revealed exactly one negative frequency; the vibration connected the two sides of the reaction. Coordinates for the calculation of all starting, intermediate, transition state and final compounds are in supporting information 9.

ASSOCIATED CONTENT

Details of the analyses are provided, and this information is available free of charge via the internet.

AUTHOR INFORMATION

Corresponding Author

*Email: kuo@lclark.edu

ACKNOWLEDGEMENT

This work was funded by NSF-RUI award CHE-1413090.

[1] N.N. Greenwood, A. Earnshaw, in: Chemistry of the Elements, Pergamon Press, Oxford, UK, 1984, pp. 1174-1184.

[2] F.A. Cotton, G. Wilkinson, in: Advanced Inorganic Chemistry, fourth ed., John Wiley & Sons, New York, 1980, pp. 472-482.

[3] J.M. Battershill, P.M. Edwards, M.K. Johnson, Food Chem. Toxicol. 42 (2004) 1279-1285.

[4] R.A. Larson, E.J. Weber, in: Reaction Mechanisms in Environmental Organic Chemistry, Lewis Press, Boca Raton, LA, 1994, pp. 122-125.

[5] J.J. Gordon, L. Leadbeater, Toxicol. Appl. Pharmacol. 40 (1977) 109-114.

[6] K. Kim, O.G. Tsay, D.A. Atwood, D.G. Churchill, Chem. Rev. 111 (2011) 5345-5403.

[7] Y. Yang, J.A. Baker, J.R. Ward, Chem. Rev. 92 (1992) 1729-1743.

[8] N.B. Munro, K.R. Ambrose, A.P. Watson, Environ. Health Perspect. 102 (1994) 18-38.

[9] M.R. Seger, G.E. Maciel, Environ. Sci. Technol. 40 (2006) 552-558.

[10] J. Bielawski, J.E. Casida, J. Agric. Food. Chem. 36 (1988) 610-615.

[11] Parathion toxicity comes from the P=S → P=O oxidation that takes place in insects and converts the applied parathion (LD_{50} = 13 mg/kg) to the more toxic paraoxon (LD_{50} = 1.8 mg/kg) [12].

T.G. Spiro, W.M. Stigliani, in: Chemistry of the Environment, Prentice Hall, Upper Saddle River, New Jersey, 1996, pp. 281-282.

[12] F. Sperling, H.K. Ewenike, T. Farber, Environ. Res. 5 (1972) 164-171.

[13] S.A. Melnychuk, A.A. Neverov, R.S. Brown, Angew. Chem. Int. Ed. 45 (2006) 1767-1770.

[14] T. Liu, A.A. Neverov, J.S.W. Tsang, R.S. Brown, Org. Biomol. Chem. 3 (2005) 1525-1533.

[15] J.S.W. Tsang, A.A. Neverov, R.S. Brown, Org. Biomol. Chem. 2 (2004) 3457-3463.

[16] A.A. Neverov, R.S. Brown, Main Group Chem. 9 (2010) 265-281.

[17] D. Marciano, M. Goldvaser, I. Columbus, Y. Zafrani, J. Org. Chem. 76 (2011) 8549-

8553.

[18] K.E. DeBruin, D.M. Johnson, J. Am. Chem. Soc. 95 (1973) 7921-7922.

[19] L.Y. Kuo, T.T. Adint, A.E. Akagi, L. Zakharov, Organometallics 27 (2008) 2560-2564.

[20] Y.C. Yang, Acc. Chem. Res. 32 (1999) 109-115.

[21] H. Morales-Rojas, R.A. Moss, Chem. Rev. 102 (2002) 2497-2521.

[22] R.A. Moss, H. Morales-Rojas, H. Zhang, B.D. Park, Langmuir 15 (1999) 2738- 2744.

[23] R. Cooper, M.L.H. Green, J. Chem. Soc. A (1967) 1155-1160.

[24] L.Y. Kuo, D.C. Baker, A.K. Dortignacq, K.M. Dill, Organometallics 32 (2013) 4759-4765.

[25] M.J. Calhorda, A.R. Dias, J.A. Martino Simoes, C. Teixeira, J. Chem. Soc., Dalton Trans. 12 (1984) 2659-2663.

[26] M.A.A.F. de C.T. Carrondo, P.M. Matias, G.A. Jeffrey, Acta Crystallogr., Sect. C: Cryst. Struct. Commun. 40 (1984) 932-934.

[27] A.R. Dias, M.H. Garcia, M.F.M. da Piedade, M.A.A.F. de C. T. Carrondo, J. Organomet. Chem. 632 (2001) 107-112.

[28] L.Y. Kuo, A.K. Bentley, Y.A. Shari'ati, C.P. Smith, Organometallics 31 (2012) 5294-5301.

[29] L.Y. Kuo, A.P. Blum, M. Sabat, Inorg. Chem. 44 (2005) 5537-5541.

[30] L.Y. Kuo, Y.A. Shari'ati, Degradation of Phosphate Esters by High Oxidation State Molybdenum Complexes, U.S. Patent 9024106 B2, May 5, 2015.

[31] G. Absillis, R.V. Deun, T.N. Parac-Vogt, Inorg. Chem. 50 (2011) 11552-11560.

[32] G. Absillis, E. Cartuyvels, R.V. Deun, T.N. Parac-Vogt, J. Am. Chem. Soc. 130 (2008) 17400-17408.

[33] B.-T. An, H.-S. Park, E.-J. Lee, I.-H. Eom, Bull. Korean Chem. Soc. 21 (2000) 905-908.

[34] P.H. Hien, K. Stroobants, T.N. Parac-Vogt, Inorg. Chem. 50 (2011) 12025-12033.

[35] H. Weil-Malherbe, R.H. Green, Biochem. J. 49 (1951) 286-292.

[36] H. Weil-Malherbe, Biochem. J. 55 (1953) 741-745.

[37] E.P. Steyn-Parvé, Biochim. Biophys. Acta 64 (1962) 13-20.

[38] D. Spencer, Aust. J. Biol. Sci. 7 (1954) 151-160.

[39] D.L. Harris, B.J. Mizock, S.J. Pilkis, J. Biol. Chem. 241 (1966) 707-714.

[40] A. dos P. Lemos, A.L.F. de Sousa, A.A.S. Pinheiro, M. Berrêdo, J.R. Meyer-Fernandes, Z. Naturforsch., C: Biosci. 57 (2002) 500-505.

[41] L.M. Franks, V. Maggi, A.W. Carbonell, J. Anat., 101 (1967) 777-787.

[42] R. van Reen, Arch. Biochem. Biophys. 53 (1954) 77-84.

[44] J.J. Cruywagen, G. Draaijer, J.B.B. Heyns, E.A. Rohwer, Inorg. Chim. Acta. 331 (2002) 322-329.

[45] M.T. Pope, in: Heteropoly and Isopoly Oxometalates, Springer Verlag, Berlin, 1983, pp. 60-117.

[46] R.W. Taft, in: M.S. Newman (Ed.), Steric Effects in Organic Chemistry, John Wiley & Sons, New York, 1956, Chapter 13.

[47] T.H. Lowry, K.S. Richardson, in: Mechanism and Theory in Organic Chemistry, third ed., Harper Collins, New York, 1987, pp. 374-375.

[48] Scifinder Substance Identifier. https://scifinder.cas.org/scifinder/view/scifinder/scifinderExplore.jsf (accessed June 20, 2016).

[49] B.R. Wikjord, L.D. Byers, J. Org. Chem. 57 (1992) 6814-6817.

[50] B. Ben-Nissan, D.D. Green, G.S.K. Kannangara, C.S. Chai, A.J. Milev, J. Sol-Gel Sci. Technol. 21 (2001) 27-37.

[51] W.-M, Wang, J.-J. Lui, L. Yao, F.-J. Meng, Y.-M. Sun, C.-Q.Zhao, Q. Xu, L.-B. Han, J. Org. Chem. (2016) 6843-6847

[52] M. Cohn, A. Hu, Proc. Natl. Acad. Sci. USA 75 (1978) 200-203.

[53] G. Lowe, B.S.J. Sproat, Chem. Commun. (1978) 565-566.

[54] H.V. Felten, B. Wernli, H.J. Gamsjäger, Chem. Soc., Dalton Trans. (1988), 496-500.

[55] T. Mihaylov, T.N. Parac-Vogt, K. Pierloot, Inorg. Chem. 51 (2012) 9619-9628.

[56] P.H. Ho, T. Mihaylov, K. Pierloot, T.N. Parac-Vogt, Inorg. Chem. 51 (2012) 8848-8859.

[57] C.-T. Chen, J.-H. Kuo, V.D. Pawar, Y.S. Munot, S.-S. Weng, C.H. Ku, C.-Y. Liu, J. Org. Chem. 70 (2005) 1188-1197.

[58] R. Sanz, M.R. Pedrosa, Curr. Org. Synth. 6 (2009) 239-263.

[59] C.S. Johnson, Prog. Nucl. Magn. Reson. Spectrosc. 34 (1999) 203-256.

[43] L.Y. Kuo, S.K. Glazier, Inorg. Chem. 51 (2012) 328-335.

[44] GaussView, Version 5, Roy Dennington, Todd A. Keith, and John M. Millam, Semichem Inc., Shawnee Mission, KS, 2016.

[45] Gaussian 09, Revision D.01, M. J. Frisch, G. W. Trucks, H. B. Schlegel, G. E. Scuseria, M. A. Robb, J. R. Cheeseman, G. Scalmani, V. Barone, B. Mennucci, G. A. Petersson, H. Nakatsuji, M. Caricato, X. Li, H. P. Hratchian, A. F. Izmaylov, J. Bloino, G. Zheng, J. L. Sonnenberg, M. Hada, M. Ehara, K. Toyota, R. Fukuda, J. Hasegawa, M. Ishida, T. Nakajima, Y. Honda, O. Kitao, H. Nakai, T. Vreven, J. A. Montgomery, Jr., J. E. Peralta, F. Ogliaro, M. Bearpark, J. J. Heyd, E. Brothers, K. N. Kudin, V. N. Staroverov, T. Keith, R. Kobayashi, J. Normand, K. Raghavachari, A. Rendell, J. C. Burant, S. S. Iyengar, J. Tomasi, M. Cossi, N. Rega, J. M. Millam, M. Klene, J. E. Knox, J. B. Cross, V. Bakken, C. Adamo, J. Jaramillo, R. Gomperts, R. E. Stratmann, O. Yazyev, A. J. Austin, R. Cammi, C. Pomelli, J. W. Ochterski, R. L. Martin, K. Morokuma, V. G. Zakrzewski, G. A. Voth, P. Salvador, J. J. Dannenberg, S. Dapprich, A. D. Daniels, O. Farkas, J. B. Foresman, J. V. Ortiz, J. Cioslowski, and D. J. Fox, Gaussian, Inc., Wallingford CT, 2013.

[46] A. Becke, J. Chem. Phys., vol. 98, pp. 5648–5652, 1993.

[47] C. Lee, W. Yang, and R. G. Parr, Phys. Rev. B, vol. 37, no.2, pp. 785–789, 1988.

[48] B. Miehlich, A. Savin, H. Stoll, and H. Pruess, Chem. Phys. Lett., vol. 157, no. 3, pp. 200–206, 1989.

[49] W. J. Hehre, R. Ditchfield, L. Radom, and J. A. Pople, J. Am. Chem. Soc., vol. 92, no. 16, pp. 4796–4801, 1970.

[50] R. Ditchfield, W. J. Hehre, and J. A. Pople, J. Chem. Phys., vol. 54, p. 724, 1971.

[51] P. C. Hariharan and J. A. Pople, Theor. Chem. Acc., vol. 28, pp. 213–222, 1973.

[52] P. J. Hay and W. R. Wadt, J. Chem. Phys, vol. 82, pp. 270–83, 1985.

[53] P. J. Hay and W. R. Wadt, J. Chem. Phys., vol. 82, pp. 299–310, 1985.

[54] V. Barone and M. Cossi, J. Phys. Chem. A, 102 (1998) 1995-2001.

[55] M. Cossi, N. Rega, G. Scalmani, and V. Barone, J. Comp. Chem., 24 (2003) 669-81.

Highlights:

- A convenient molybdate that catalytically hydrolyzes phosphonothioate neurotoxins under mild aerobic conditions
- Phosphonothioate hydrolysis is accomplished with desired P-S bond scission to yield non-toxic phosphonate product
- A proposed mechanism uses the molybdate as an oxoanion-nucleophile to carry out an $S_N2(P)$ on the phosphonothioate.

GRAPHICAL ABSTRACT

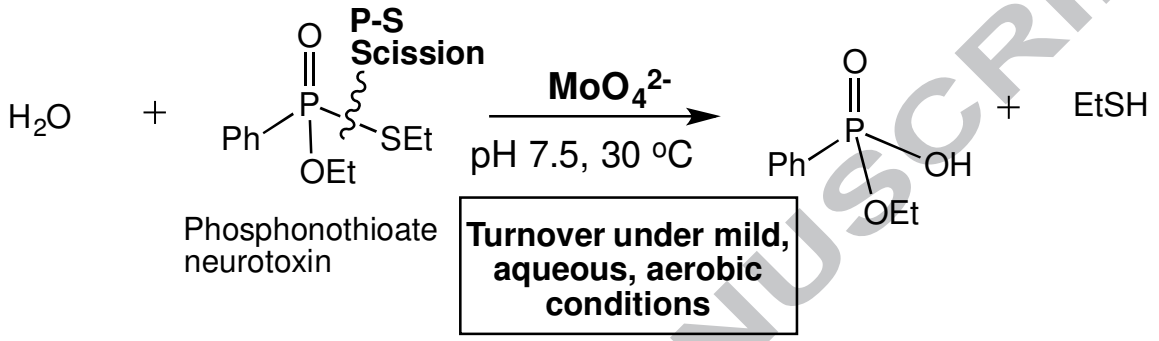

A phosphonohioate is catalytically hydrolyzed with specific P-S bond scission by a simple molybdate under mild aqueous conditions (pH 7.5, 30 °C). Catalyst (MoO_4^{2-}(*aq*)) loading as low as 15% achieved complete hydrolysis of the phoshonothioate neurotoxin which served as a mimic for the chemical warfare agent VX.